Bubble functionalization in flotation process improve microalgae harvesting

Irem Demir-Yilmaz, Malak Souad Ftouhi, Stéphane Balayssac, Pascal Guiraud, Christophe Coudret, Cécile Formosa-Dague

Bubble functionalization in flotation process improve microalgae harvesting

Irem Demir-Yilmaz,[1,2] Malak Souad Ftouhi,[1] Stéphane Balayssac,[3] Pascal Guiraud,[1,4] Christophe Coudret,[3,4] and Cécile Formosa-Dague[1,4*]

[1] TBI, Université de Toulouse, INSA, INRAE, CNRS, Toulouse, France.

[2] LAAS, Université de Toulouse, CNRS, Toulouse, France.

[3] UMR 5623 IMRCP, CNRS, Toulouse, France.

[4] Fédération de Recherche Fermat, CNRS, Toulouse, France.

*corresponding author: Cécile Formosa-Dague, formosa@insa-toulouse.fr

Abstract

Microalgae are a promising resource for biofuel production, although the lack of effective harvesting techniques limits their industrial use. In this context, flotation, and in particular dissolved air flotation (DAF), is an interesting separation technique that could drastically reduce harvesting costs and make biofuel-production systems more economically viable. But because of the repulsive interaction between cells and bubbles in water, the efficiency of this technique can be limited. To solve this problem, we propose here an original DAF process where bubbles are functionalized with a bio-sourced polymer able to specifically bind to the surface of cells, chitosan. In a first part, we modify chitosan by adding hydrophobic groups on its backbone to obtain an amphiphilic molecule, PO-chitosan, able to assemble at the surface of bubbles. Then, using a recently developed technique based on atomic force microscopy (AFM) combined with microfluidics, we probe the interactions between PO-chitosan coated bubbles and cells at the molecular scale; results show an enhanced adhesion of functionalized bubbles to cells (from 3.5 to 12.8 nN) that is pH-dependent. Separation efficiencies obtained in flotation experiments with functionalized bubbles are in line with AFM data, and a microalgae separation efficiency of approximately 60% could be reached in a single step. In addition, we also found that PO-chitosan could be used efficiently as a flocculant (nearly 100% of cells removed), and in this case AFM experiments revealed that the flocculation mechanism is based on hydrophobic interactions between cells and PO-chitosan. Altogether, this comprehensive study shows the interest of PO-chitosan to harvest cells in flotation or flocculation/flotation processes.

Keywords: Flotation, Flocculation, Functionalized bubbles, Chitosan, Atomic force microscopy, Microalgae

1. Introduction

Microalgae are photosynthetic microorganisms capable of capturing sunlight and converting carbon dioxide into value-added products such as biofuels, dietary products and animal feed. [1]. For biofuel production, microalgae are currently considered the most promising biomass due to their many advantages over terrestrial plants, such as rapid growth, high capacity to accumulate lipids under certain conditions and the possibility of growing them on non-arable land [2]. Despite these advantages, broad commercialization of microalgae-sourced biodiesel has been restrained due to the high costs involved in production processes. Basically, biofuel production from microalgae can be divided into the following major steps: cultivation, harvesting, extraction and down-stream processes [3]. The most expensive of these steps is the harvesting of microalgae; as they grow at low concentration (0.3–3 g/L), large volumes of water need to be treated to recover small quantities of biomass [4]. Although the choice of microalgae harvesting technique depends largely on the microalgae species and the desired end product, the most commonly used techniques are centrifugation, filtration and sedimentation [5]. These methods however are generally associated with a low efficiency, high capital costs and important energy and/or chemicals consumptions. For example, centrifugation requires a high energy input (up to 8 kWh/m^3 of microalgae, [6]) which represents a huge cost for largescale processing, and may also damage cells due to the high shear forces, resulting in a significant loss of the products of interest [1]. Likewise permeable membranes used for filtration are easily clogged by small microalgae [7], which also leads to important processing costs and material costs.

In this context, flotation could be an interesting alternative harvesting technique as it is a proven technology to efficiently capture small particles in an aqueous solution using air bubbles. In this way, it takes advantage of the natural characteristics of microalgae, namely a relatively low density and a tendency to self-flotation [8]. In addition, because it is a relatively rapid operation, with low space requirements, high flexibility and moderate operational costs, flotation technique has the potential to overcome the bottleneck of feasible microalgal biofuel production [9]. Indeed, when combined to a flocculation step, the energy demand reported can be as low as 1.5 kWh/m^3 [10]. However, its efficient use for microalgae harvesting is still challenging as cells are usually negatively charged. The surface of air bubbles being also negatively charged in water, [11] they repeal each other preventing adhesion and thus capture and flotation. To improve flotation efficiency, adding a flocculation step prior to flotation can be a good solution. Synthetic flocculants added to the microalgal suspension aggregate cells into large flocs that can be easily captured by the bubbles [12]. However, contamination is a major issue in this technique as flocculants at the end of the process end up in the harvested biomass and can have an important impact on the final quality of the products [9]. To avoid this problem, natural flocculation is a preferred alternative. So far, two types of natural flocculation mechanisms have been identified: auto-flocculation, where flocculation is triggered by a molecule or precipitate that forms naturally in the culture medium, and bio-flocculation, where a molecule produced by cells is directly responsible for flocculation [13]. But because natural flocculation can be difficult to control or trigger in industrial processes, many studies have showed the interest of using bio-flocculants like biopolymers either directly extracted from other organisms like natural polysaccharides, or modified by various means to control the functional chemical groups they present and induce natural flocculation [14–17]. The most popular biopolymer used for microalgae harvesting is with no doubt chitosan. Chitosan is a cationic polyelectrolyte at pH lower than its pKa (6.5) obtained by deacetylation of chitin. After cellulose, it is the second most abundant natural polymer on earth [18,19]. Moreover as chitin-like polysaccharides are naturally present in the cell wall of several microalgae species [20], chitosan does not contaminate the harvested biomass. To understand its flocculation mechanism, our team recently performed atomic

force microscopy (AFM) experiments to probe the interactions between chitosan and cells. AFM, first developed in 1986, is a powerful tool that can be used to study microalgae cells at the nanoscale and characterize their interactions with their environment [21]. The results obtained in this study showed that at low pH, chitosan is able to form specific interactions with polymers present at the surface of cells, in this case, cells of *Chlorella vulgaris*, while at higher pH, chitosan forms a precipitate in which cells get entrapped [17].

Another possibility to improve the efficiency of flotation for microalgae harvesting that has been explored is to modify the surface of the bubbles. The principal example of such a strategy was provided by Henderson's team, who modified the surface of the bubbles with positively charged polymers, thereby changing the charge of the bubbles and making interaction with the cells attractive. Using this strategy named Posi-DAF (positive dissolved air flotation), the authors could obtain a maximum separation efficiency of 97%, 54% and 89% in the case of *Melosira aeruginosa*, *C. vulgaris* and *Asterionella formosa* cells respectively. Here in this work, we also propose a bubble-modification strategy, based on the recent findings that we generated on the mechanism of interaction of chitosan with cells [17]. The hypothesis is that since chitosan is able to bind specifically to microalgae cells at low pH, if we functionalize it at the surface of bubbles, then flotation separation could be efficient without the need of a flocculation step. Removing this step in a large-scale production system could result in reduced costs, reduced harvesting time, and could represent an important step forward for the use of microalgae for biofuel production. This is what is presented in this study, and for that we worked with a biotechnologically-relevant freshwater microalgae species, *C. vulgaris*. The first step of this work was to modify chitosan so it could be functionalized at the surface of bubbles, by adding hydrophobic groups on its hydrophilic backbone. Then, using a recently developed approach based on FluidFM technology, which combines AFM and microfluidics, we could probe the interactions between functionalized bubbles and cells at the molecular scale, and this way understand the mechanism involved in this interaction [22]. Finally, the effectiveness of this original flotation process in different experimental conditions was determined. But as we were investigating the interacting behavior of this chitosan-based molecule, we also found that it could be successfully used as a flocculant; AFM experiments in this case allow understanding how the modifications made on chitosan affected the physico-chemical basis of its interactions with cells. Altogether, this work has led to the development of an original flotation process based on functionalized bubbles with a modified chitosan molecule, which can also serve as a flocculant depending on the application and needs. Finally the AFM experiments performed at the molecular scale could highlight the mechanisms at play, thereby giving a full understanding of the interaction mechanisms involved in both cases.

2. Materials and methods

2.1. Chemicals.

Chemicals for the synthesis of alkyl-chitosan derivatives were the following: chitosan (from shrimp, practical grade, ≥ 75% degree of deacetylation, C3646), octanal (O5608), sodium hydroxide (S0899), sodium cyanoborohydride reagent grade 95% (156159), Deuterium chloride solution (543047) were purchased from Sigma-Aldrich as well as glacial acetic acid 99.5% (W200611) and ethanol 96% (1.59010) and used as received.

2.2. Synthesis and characterization of polyoctyl chitosan (PO-chitosan).

The N-octyl-chitosan derivatives were obtained by reductive amination following a procedure previously described in the literature [23–26]. In brief, 6 g of chitosan were dissolved in 450 mL of 0.2 M acetic acid (AcOH) to which was added 180 mL of ethanol after compete dissolution. The pH was adjusted to 6 with 4 M of NaOH to prevent macromolecule precipitation. A solution of octanal (target alkylation level of 10%) in 40% of ethanol was added using a 1:3 ratio prior to adding an excess of sodium cyanoborohydride ($NaBH_3CN$) (3:1 mole ratio per glucosamine monomer). After stirring for 24h at room temperature, the pH of the reaction mixture was adjusted to 7-8 using a solution of 4 M of NaOH. The precipitate was collected by centrifugation for 5 min at 6000 rpm at 4°C and was then thoroughly washed with ethanol/water mixture at least 5 times with increasing ethanol concentration from 40% (v/v) to 100% (v/v) before drying until constant weight. NMR spectroscopy was used to characterize both chitosan and N-octyl-chitosan derivatives produced to determine the degree of substitution (DS). The NMR spectra were performed on a Bruker Advance spectrometer (Bruker, Switzerland) in D_2O-DCl (pH around 4) at a resonance frequency of 400.13 MHz and 70°C on the starting material and on the final product. The degree of substitution was calculated from NMR spectra as previously described elsewhere [23]. Integration of the anomeric protons and acetyl groups were obtained using the TOPSPIN 4.0.8 software (Bruker, Switzerland) and gave an acetylation degree of 20% (consistent with the starting material), 12% of octylated monomers, and 68% of free amine monomers.

2.3. Microalgae strain and culture.

The green freshwater microalgae *Chlorella vulgaris* strain CCAP 211/11B (Culture Collection of Algae and Protozoa, Scotland, UK) was cultivated in sterile conditions in Wright's cryptophyte (WC) medium prepared with deionized water, as previously described [17]. Cells were cultivated at 20°C, under 120 rpm agitation, in an incubator equipped with white neon light tubes providing illumination of approximately 40 µmol photons m^{-2} $s^{-1,}$ with a photoperiod of 18h light: 6h dark. Exponential phase experiments were performed with 7-day batch cultures, while stationary phase and salinity stress condition (0.1M NaCl) experiments were performed with 21-day batch cultures.

2.4. Roughness analyses.

Roughness analyses were performed on PO-chitosan immobilized on glass slides. PO-chitosan was functionalized at the surface of glass slides using spin-coating, according to a procedure described in Demir *et al.* 2020 [17]. Briefly, 2.5 g/L PO-chitosan (pH around 2 adjusted with HCl) solution was deposited on a clean glass slide and spin-coated at 1000 rpm for 3 min. The glass slides were then dried in an incubator at 37°C overnight before use. Height images of the PO-chitosan surfaces were

recorded in PBS at pH 6, 7.4 and 9 using contact mode available on the Nanowizard III AFM (Bruker, USA), and MSCT cantilevers (Bruker, nominal spring constant of 0.01 N/m). Images were recorded with a resolution of 256 x 256 pixels using an applied force < 1 nN. In all cases the cantilevers spring constants were determined by the thermal noise method prior to imaging [27]. The height images obtained were then analyzed using the Data Processing software (Bruker, USA) to determine the arithmetic average roughness (Ra) of 6 different areas of 25 μm^2 (5 µm x 5 µm) for each sample.

2.5. Flocculation and flotation experiments.

Flocculation and flotation separation of *C. vulgaris* was performed in a dissolved air flotation (DAF) homebuilt flotation device, described elsewhere [28]. Briefly, the depressurization at atmospheric pressure of water saturated by air at 6 bars induced the formation of bubbles. Water free of algae was pressurized for 30 min before injection into the jars. The injection was controlled by solenoid valves and a volume of pressurized water was added to each beaker sample. Two types of experiments were conducted, repeated 3 times for each condition with cells coming from 2 independent cultures:

- Flocculation: *C. vulgaris* cells were cultured during 7 days until they reached mid-exponential phase. Then 100 mL of cell suspension was directly poured into the test-jars with an initial optical density (OD) at 750 nm of 0.8. Flocculants, chitosan and PO-chitosan, were directly added (final concentration of 10, 15 and 20 mg/L for chitosan and of 12, 17, 22, 25, 30, 40 and 60 mg/L for PO-chitosan) to the suspension, which was stirred at 100 rpm for 20 minutes to homogenize and left to settle for 30 minutes. OD at 750nm of the suspension was measured afterwards to calculate flocculation efficiency.
- Flotation: *C. vulgaris* cells were cultured during 7 days until they reached mid-exponential phase. Then, 100 mL of cell suspension was directly poured into the test-jars with an initial OD_{750} of 0.8. PO-chitosan mixed with water was directly added to the pressurization tank (final concentration of 30, 25 and 20 mg/L); the mix was then pressurized during 30 minutes at 6 bars. Following this, depressurization at atmospheric pressure of the water-PO-chitosan mix saturated by air was performed to inject functionalized microbubbles into each flotation beaker (bubble volume of 20, 50, 80 and 100 mL). The algal suspension was retrieved from the bottom of the test-jars: 30 mL were used for quantifying flotation efficiency.

For both types of experiments, the optical density of the withdrawn microalgae suspension (OD_f) was measured and compared to the optical density of the microalgae suspension measured before the experiments (OD_i), taking the initial and final volumes into account (V_i and V_f). The flotation efficiency (E) was calculated according to the following equation 1.

$$E = \frac{OD_i.V_i - OD_f.V_f}{OD_i.V_i} \quad (1)$$

2.6. Zeta Potential Experiments.

The global electrical properties of *C. vulgaris* cell surface at pH 6, 7.4 and 9 were assessed by measuring the electrophoretic mobility with an automated laser zetameter (Zetasizer NanoZS, Malvern Instruments). To this end, microalgae were harvested by centrifugation (3000 rpm, 3 min), washed two times in PBS at a pH of 6, 7.4 or 9, and resuspended in the same solution at a final concentration of 1.5×10^6 cell/mL. For each condition, analysis were performed in triplicate.

2.7. Granulometry analysis.

Particle size distributions of both chitosan and PO-chitosan were determined using a Mastersizer (Malvern Instruments, UK). For that, PO-chitosan was dissolved in water with a pH around 2 (with HCl) and stirred for 1 week at final concentrations of 2.5 g/L, 1 g/L and 0.5 g/L. The refractive index used for micelles was of 1.350. The results are presented as an average number obtained from 3 measurements.

2.8. Force spectroscopy experiments using FluidFM technology.

Force spectroscopy experiments were conducted using a NanoWizard III AFM (Bruker, USA), equipped with FluidFM technology (Cytosurge AG, Switzerland). In each case, experiments were performed in PBS at pH 6, using micropipette probes with an aperture of 2 µm (spring constant of 0.3, and 4 N/m, Cytosurge AG, Switzerland). First, PBS at a pH of 6 was used to fill the probe reservoir (5 µL); by applying an overpressure (100 mBar) the PBS then filled the entire cantilever microchannel. The probe was then immersed in PBS and calibrated using the thermal noise method prior to measurement [27]. A single *C. vulgaris* cell was then aspirated from the surface of the Petri dish by approaching the FluidFM probe and applying a negative pressure (−200 mBar). The presence of the cell on the probe was verified by optical microscopy. The cell probe was then used to measure the interactions with PO-chitosan immobilized on glass slides. Interactions between single *C. vulgaris* cells aspirated at the aperture of FluidFM cantilevers and PO-chitosan were recorded at pH 6, 7.4 and 9 at a constant applied force of 1 nN, force curves were recorded with a z-range of up to 2 µm and a constant retraction speed of 2.0 µm/s to 4 µm/s. Data were analyzed using the Data Processing software from Bruker. Adhesion forces were obtained by calculating the maximum adhesion force for each retract curves. Results were recorded on ten different cells coming from at least two independent cultures.

2.9. Bubble formation and functionalization using FluidFM.

Air-bubbles were formed using FluidFM as described in Demir *et al*. [22], using a Nanowizard III AFM (Bruker, USA), equipped with FluidFM technology (Cytosurge AG, Switzerland). Experiments were performed in PBS, using microfluidic micropipette probes (FluidFM cantilevers) with an aperture of 8 µm (spring constant of 0.3 and 2 N/m, Cytosurge AG, Switzerland). Briefly, hydrophobized FluidFM cantilevers were first filled with air and immersed in PBS. A single bubble was then formed at the aperture of the cantilevers by applying a positive pressure (200 mbar) inside the cantilever thanks to the pressure controller to which it is connected. To produce functionalized bubbles, the FluidFM cantilever was immersed in a solution of 2 mg/L of PO-chitosan. This solution was aspirated inside the cantilever by gradually decreasing the pressure from 0 mbar to -200 mbar. After that the FluidFM cantilever containing the surfactant solution was immersed in PBS buffer without surfactants. By increasing the pressure to 150 mbar, the surfactant solution was then locally dispersed in the buffer and a bubble was formed: the surfactant then assembled at the surface of the produced bubble. Interactions between PO-chitosan coated bubble produced at the aperture of FluidFM and single *C. vulgaris* cells were recorded at pH 6, 7.4 and 9 at a constant applied force of 1 nN, force curves were recorded with a z-range of up to 2 µm and a constant retraction speed up to 4 µm/s.

2.10. Statistical analysis.

Experimental results represent the mean ± standard deviation (SD) of at least three replicates. For each experiments, the number of replicates is indicated in the results and discussion section. For large samples, student t-test was used to assess the difference observed in the results. For small samples (less than 20) Mann and Whitney test was used to assess the difference. The differences were considered significantly at $p < 0.05$.

3. Results and Discussion

3.1. Synthesis of PO-chitosan

The first step of this study consisted in the synthesis of PO-chitosan using the reductive amination reaction illustrated in Figure 1a. Such reaction preserves the number of basic nitrogens and can be performed under mild conditions that do not modify the chitosan molecule itself (degree of acetylation and/or polymerization degree) as described elsewhere [24]. Octanal was chosen as a precursor of the hydrophobic alkyl groups, this way the amphiphilic character of the target molecule PO-chitosan can be reached without the complete alkylation of all glucosamine monomers and indeed a 10% stoichiometric ratio is sufficient. Thus, some of the primary amino groups of chitosan undergo a Schiff reaction with octanal to yield the corresponding aldimines, which are then converted to alkyl derivatives by reduction with $NaBH_3CN$. ^{1}H-NMR spectroscopy in D_2O/DCl (pH ~ 4) at 70°C was used to characterize both chitosan and PO-chitosan and determine the degree of substitution (DS) of the amine functions by the octyl chains. The ^{1}H-NMR spectra of initial chitosan and PO-chitosan are presented in Figure 1b and c respectively. The octyl chain in PO-chitosan can be easily identified by the signals in the 0.7 – 1.7 ppm region. Thus, the signal at 0.7 ppm was attributed to the terminal -CH_3 while those at 1.6 ppm and the multiplet at 1.1-1.3ppm, to respectively the -CH_2 group linked to the N atom and the core CH_2 of the octyl chain.

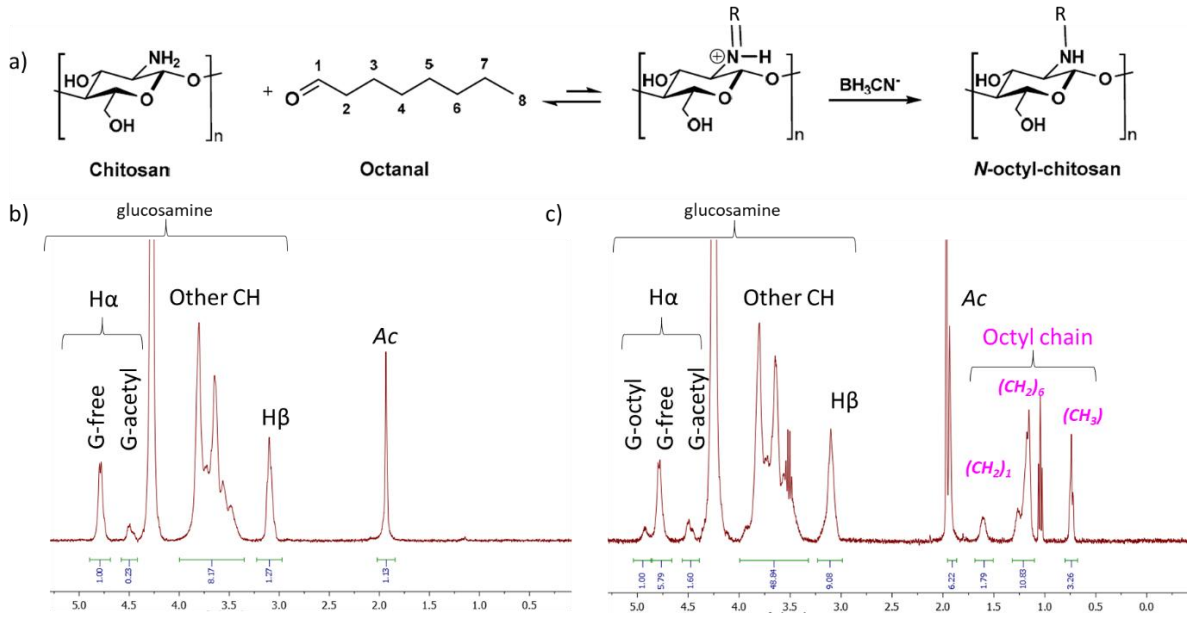

Figure 1. Synthesis of PO-chitosan. *a) Synthesis of PO-chitosan by alkylation, b) ^{1}H-NMR spectra obtained for initial chitosan, c) ^{1}H-NMR spectra obtained for PO-chitosan. The DS obtained for PO-chitosan is of 12%.*

The degree of substitution was calculated as previously described [23], by examining the relative integration of the anomeric protons Hα , using the assignation previously reported [23–25].

* at 4.54 ppm, the acetylglucosamine unit,
* at 4.80 ppm, the unsubstituted glucosamine unit
* at 4.94 ppm, the monosubstituted glucosamine unit.

It was found to be of 12% (Figure 1c), meaning that 12% of the amine functions of chitosan have been modified with octanal molecules. This number is close to the targeted degree of substitution (10%) and to what was found by Mati-Baouche *et al.* who described the reaction in these specific conditions [24]. The relative number of N-acetylated glucosamine remained unchanged compared to the starting chitosan confirms the mildness of the reaction conditions used.

3.2. Characterization of PO-Chitosan using atomic force microscopy

PO-chitosan has already been characterized on the basis of its water resistance, rheological characteristic and bonding properties to wood and aluminum surfaces [24,25]. Here we characterized PO-chitosan on the basis of its surfactant properties, particle size, roughness and hydrophobicity, which are parameters important to then optimize the next experiments of this study (AFM, flocculation and flotation experiments). PO-chitosan has both hydrophilic (-NH_2 or –OH) and hydrophobic sites (alkyl chains, octanal), and thus possess amphiphilic properties, making it a surfactant. As for any surfactants, it should be able to decrease the surface tension of water with increasing concentration. Surface tension experiments were then performed, the results are presented in Supplementary Figure 1. They show that with increasing concentration of PO-chitosan, the surface tension of water decreases from approximately 72 to 62 mN/m for a PO-chitosan concentration of 2.5 g/L. This decrease as important as it can be with other types of surfactants, but this can be explained by the degree of substitution of the molecule, which is of 12%. This means that only 12% of the amine functions of chitosan have been modified with hydrophobic octanal molecules, thus the hydrophobic part of the molecule may not be large enough to change in an important manner the surface tension of water. However, in order to be able to dissolve the molecule in water, there needs to be a balance between the hydrophobic and hydrophilic groups. For instance, for low molecular weight chitosan, even with a substitution degree of 10%, the resulting molecule is water insoluble. Whereas, for high molecular weight chitosan we are limited with low alkylation level (10-15 %) because as the alkylation level increases, water solubility of PO-chitosan decreases, and we need water soluble compounds to use for the next experiments. To verify we can completely dissolve PO-chitosan in water, we measured the particle size of both initial chitosan and PO-chitosan in water using granulometry. The size distribution graphs obtained are shown in Supplementary Figure 1b and c respectively (concentration of 2.5 g/L). They both show a similar pattern which means that the addition of octanal does not modify the size of chitosan significantly (high molecular weight).

Moreover, we also measured the turbidity of chitosan and PO-chitosan solutions at different concentrations (2.5, 1 and 0.5 g/L): the obtained turbidities are of 4.3, 3.2 and 3.5 NTU respectively. This means that solutions are clear (NTU < 5 corresponds to clear water). Thus both size measurements and turbidity experiments prove that we are able to dissolve PO-chitosan in water. Moreover, based on the literature we know that chitosan and PO-chitosan behave differently. For example, rheological analysis show that alkyl-chitosan solutions are non-Newtonian fluids, since the viscosity decreases with increasing shear rate whereas initial chitosan shows a Newtonian behavior [23–25]. Further, Desbrieres *et al.* highlighted that addition of octanal or increase in the DS, is linked with the increase in viscosity of PO-chitosan since the intermolecular hydrophobic interaction is a key element in physico-chemical (rheological) properties of the modified chitosan. The higher the hydrophobic properties (the length of the alkyl chain or degree of substitution) of macromolecular chain the larger the gap to the Newtonian behavior [25]. Thus, more analysis needs to be performed

on PO-chitosan to understand the differences with chitosan, such as roughness and hydrophobicity measurements.

Regarding the hydrophobic properties of PO-chitosan, it has been found that pH has an influence on the hydrophilic and hydrophobic balance of the molecule due to the ability of $-NH_2$ functions (hydrophilic part) to be ionized in acidic conditions [23]. We thus measured the hydrophobicity of PO-chitosan at different pH (pH 6, 7.4 and 9) relevant for flocculation or flotation processes for *C. vulgaris* cells, using a method recently developed in our team based on the interactions between bubbles produced by FluidFM and samples [22,29]. Air bubbles in water behaving like hydrophobic surfaces, by measuring their direct interactions with surfaces it is possible to determine the hydrophobic properties of the samples in terms of adhesion force, and further convert these forces into water contact angles (WCA) [22]. Using WCAs values we can then compare our data directly to the ones available in the literature. To perform these experiments, PO-chitosan was immobilized on glass slides by spin coating and their interaction with bubble were measured in PBS buffer at pH 6, the pH generally used for chitosan induced flocculation, pH 7.4, the optimum pH for *C. vulgaris* growth, or pH 9 which corresponds to the pH *C. vulgaris* cultures reach after 7 days. A schematic representation of these measurements is presented in Figure 2a. The adhesion force histograms obtained at pH 6, 7.4 and 9 are presented in Figure 2b, c and d respectively. In each case the force curves obtained show a single peak occurring at the contact point (inset in Figure 2b, c and d), which is characteristic of non-specific interactions such as hydrophobic interactions [30]. On each force curve obtained, the adhesion force is then quantified by measuring the height of this adhesion peak, which corresponds to the force needed to break the interaction between the bubble and the sample. This force reflects the degree of hydrophobicity of the sample, the stronger the adhesion, the higher the hydrophobicity. In the case of pH 6, the average adhesion force is of 66.7 ± 13.9 nN (Figure 2b, n= 3125 force curves obtained on 5 different measurements). While this value stays similar at a pH of 7.4 (64.6 ± 20.3 nN, Figure 2c, n = 1977 force curves obtained on 5 different measurements), it decreases to 46.5 ± 15.9 nN at pH 9 (Figure 2d, n = 1454 force curves obtained on 5 different measurements). Even though the average adhesion values at pH 6 (66.7 ± 13.9 nN) and 7.4 (64.6 ± 20.3 nN) are close to each other, statistical analysis shows that they are significantly different (p-value of 0.05, unpaired student test). The conversion of these adhesion values into WCAs gives the results presented in Table 1, which show that indeed, pH has an effect on the hydrophobicity of the molecule, as the WCA decreases with increasing pH values. The important point to note as well in this case is that initial chitosan is completely hydrophilic (WCA of 0) and does not interact with bubbles (Supplementary Figure 2) whatever the pH considered; it is the modifications made on the molecule and the addition of octanal that confers amphiphilic properties to PO-chitosan.

Table 1. Hydrophobic properties of PO-chitosan at different pH. *Adhesion values obtained by FluidFM and corresponding water contact angle (WCA) of chitosan and of PO-chitosan surfaces at pH 6, 7.4 and 9.*

Sample	pH	Adhesion value (nN)	WCA (°)
Chitosan	6	0	~ 0
	7.4	0	~ 0
	9	0	~ 0
PO-chitosan	6	66.7 ± 13.9	48.7
	7.4	64.6 ± 20.3	48.3

	9	46.5 ± 15.9	44.6

Previous studies have showed that chitosan, at elevated pH, precipitates into the medium [16,17]. This precipitation was visible when we imaged in a previous study chitosan coated surfaces using AFM, where aggregates of chitosan formed on the surface, resulting in an increased roughness (13 ± 5 nm) compared to low pH (0.6 ± 0.1 nm) [17]. To check whether PO-chitosan behaves like chitosan at high pH, we further characterized it by imaging PO-chitosan surfaces at pH 6, 7.4 and 9 using AFM in contact mode. The height images obtained are presented in Figure 2e, f and g respectively, they show a similar topography in all cases, with no aggregates present on the surface. The quantification of the surface roughness in each case gave similar values (box plot in Figure 2k), with a roughness of 574.0 ± 105.7 pm at pH 6, of 528.1 ± 144.8 pm at pH 7.4 and of 494.1 ± 82.2 pm

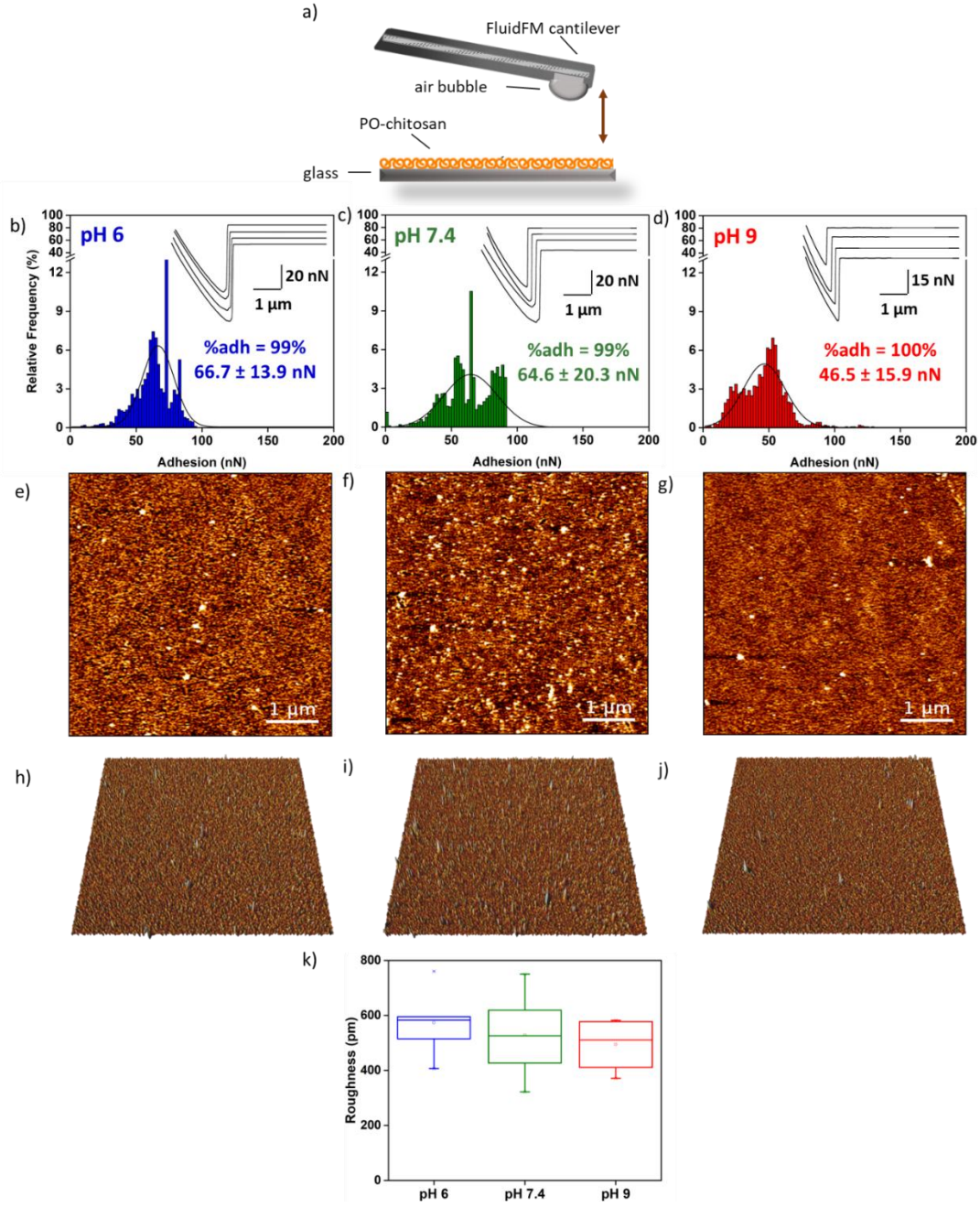

at pH 9. Non-parametric statistical tests (Mann and Whitney test) showed that these values indeed are not significantly different. These results confirm the observations from the height images, whatever the pH, PO-chitosan surfaces are homogeneous with no aggregates formed, meaning that PO-chitosan does not precipitate at high pH like chitosan does.

Figure 2: Characterization of PO-chitosan surface at different pH. *a) Schematic representation of bubble and PO-chitosan surface interaction. Adhesion force histogram obtained between bubble and PO-chitosan surface at b) pH 6 c) pH 7.4 and d) pH 9. AFM height images of PO-Chitosan surface at e) pH 6 (color scale = 4 nm) f) pH 7.4 (color scale = 4 nm) and g) pH 9 (color scale = 4 nm) and their corresponding 3D AFM vertical deflection images h) pH 6 i) pH 7.4 and j) pH 9. k) Quantification of PO-chitosan surface roughness at different pH.*

Thus, in summary, the modification of chitosan by addition of hydrophobic octanal molecules on its backbone, with a DS of 12%, made it amphiphilic as confirmed by surface tension experiments that showed a decrease in the surface tension. The new molecule PO-chitosan can also be completely dissolved in water, as confirmed by particle size and turbidity measurements. Then, using FluidFM experiments, we showed that the modifications made indeed changed the hydrophobic properties of the molecule, which are dependent on the pH, as described in the literature. Finally AFM measurements showed that PO-chitosan, unlike chitosan, does not precipitate at elevated pH. Now the next step of this study is to functionalize it at the surface of bubbles and determine if this functionalization allows a better adhesion of bubbles with cells.

3.3. PO-chitosan functionalized bubbles improve flotation efficiency

The characterization of PO-chitosan has showed that the molecule is indeed amphiphilic, able to act like a surfactant, thus we can use it to coat the surface of bubbles. The question is now to know if the presence of PO-chitosan on the surface of bubbles improves its adhesion to cells, and by which mechanism. To verify this point, we modified the surface of bubbles produced with FluidFM with PO-chitosan (concentration of 2 mg/L) using a protocol previously developed in our team [22]. Briefly, for that, a solution containing PO-chitosan is first aspirated inside a FluidFM cantilever. The cantilever is then immersed in the petri dish containing cells: by applying a positive pressure, the PO-chitosan solution is released, a bubble is formed, and because PO-chitosan molecules are in close proximity of the bubble, they directly assemble at its surface. PO-chitosan coated bubbles can then be used to probe the direct interactions with *C. vulgaris* cells. The results are presented in Figure 3. Figure 3a is a schematic representation of the experimental set-up. In this case the retract force curves obtained showed a single retract peak at the contact point (red curve in Figure 3b) with an average adhesion force of 12.8 ± 1.5 nN at pH 6 (Figure 3c in dark blue, n= 3603 force curves from 7 different cells coming from 2 independent cultures). This interaction is 3.6 times higher than the one obtained between clean bubbles and cells (Figure 3c in light blue), meaning that indeed, the functionalization of the bubble surface with PO-chitosan enhances the direct interaction with *C. vulgaris* cells. Moreover, the approach force curve also shows a “jump-in” peak reflecting the fact that the PO-chitosan coated bubble gets suddenly attached to the *C. vulgaris* cell (Figure 3b, blue curve). This jump-in, as previous studies on bubble-hydrophobic surface interaction show [22], is most likely due to the long-range hydrophobic force that causes the disruption of the water film and the formation of the three phase contact (TPC) line. This is an important point. Indeed, when we characterized the interactions between chitosan and *C. vulgaris* cells in our previous study, the force curves obtained showed multiple peaks taking place away from the contact point, materializing the unfolding of polymers from the surface of cells upon retraction [17]. In theory, the hydrophobic parts of PO-chitosan should be inside the air bubble, while the rest of the chitosan molecule, which is hydrophilic, should be outside the bubble, available for interaction. Thus, we expected to obtain the same interactions with PO-chitosan coated bubbles as we had with chitosan alone. This is clearly not the case, and our hypothesis to explain this is that when the coated bubble contacts the cell, the specific interaction between the hydrophilic backbone of the chitosan and the cell can take place, but because this interaction is effective, the water film between the bubble and the cell breaks down, resulting in the formation of the TPC line. At this point, when the bubble probe is retracted from the

cell, the hydrophobic interaction becomes dominant over the specific interaction, and this is what we see on the force curve. The fact that this hydrophobic force is much higher in the case of PO-chitosan coated bubbles compared to clean bubbles can be explained by the first attractive specific interaction of the cells with the hydrophilic backbone of the chitosan present on the bubble surface. In addition, the formation of the TPC line increases the contact area between the bubble and the *C. vulgaris* cells, which increases the adhesion forces obtained. For example, in our previous study we already prove that there is a direct relationship between effective radius (thus the contact area) and hydrophobic forces. Meaning that increase in hydrophobicity enhances the effective radius between hydrophobic surfaces and bubble due to the TPC line formation thereby leading to higher adhesion forces [22].

We further repeated these experiments at pH 7.4 and 9 (Figure 3d and e). At pH 7.4, cells interact more with clean bubbles with an average adhesion force of 4.0 ± 1.2 nN (Figure 3d, light green histogram, n= 2814 force curves from 5 cells) compared to pH 6, which can be explained by some changes perhaps in the hydrophobicity of *C. vulgaris* cells surface at this pH. When bubbles are functionalized with PO-chitosan, the average force obtained is of 4.6 ± 1.4 nN (Figure 3d, dark green n= 2814 force curves from 5 cells), thus almost 3 times less than at pH 6. In addition in this case, the "jump-in" peak on the approach curves was not visible anymore. This important decrease in the adhesion is most probably due to the decrease in the hydrophobicity of PO-chitosan molecule. Although this decrease is low, it has important consequences on the interactions with cells. At pH 9 (Figure 3e), cells do not interact with clean bubbles (0% of adhesion, light red bar in Figure 3e) at all, while when bubbles are coated with PO-chitosan, the percentage of force curves showing retract adhesions is of 23%, with an average force of 0.3 ± 0.1 nN (dark red histogram in Figure 3e, n=4419 from 7 cells coming from 2 independent cultures). In the case of chitosan, there was no interaction with cells at higher pH, but this was explained by the fact that chitosan precipitated at such pH values. The roughness measurements performed in the first part of this work showed that PO-chitosan does not precipitate like chitosan does at higher pH. Therefore, this lack of interaction is probably not related to PO-chitosan, but to the cell surface itself. Indeed, in this case, clean bubbles do not interact with cells, which means that at pH 9, the cell surface is completely hydrophilic. This can be explained by a change in the cell wall composition at higher pH [20], or by a change in the cell surface architecture where hydrophobic molecules at the surface of cells may be masked by other components [17]. Thus, the initial interaction between the hydrophilic chitosan backbone at the surface of bubbles still takes place, as proven by the low adhesions recorded. However, because the cell surface is hydrophilic, the liquid film between the bubbles and the cells cannot be broken, resulting in a weak adhesion force. These results are important because they provide insight into the molecular mechanism underlying the interactions of PO-chitosan bubbles with cells. While the interaction with PO-chitosan bubbles probably starts with a specific interaction between the chitosan molecules present at the surface of bubbles and cell surface polymers, hydrophobicity remains the main factor allowing then the contact between bubbles and cells.

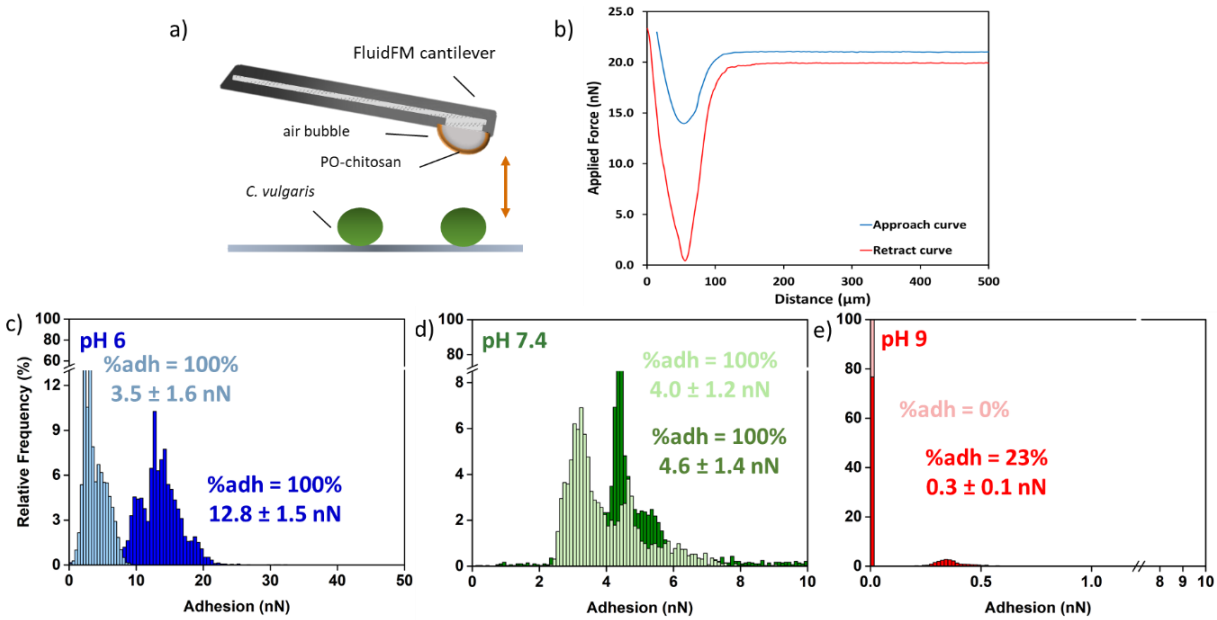

Figure 3: Modulation of the interactions between bubbles and C. vulgaris cells by PO-chitosan. *a) Schematic representation of PO-chitosan coated bubble and single C. vulgaris cell interaction. b) Representative force curves obtained for PO-chitosan coated bubble and C. vulgaris cell at pH 6. Adhesion force histogram obtained for the interactions between PO-chitosan coated bubbles and C. vulgaris cell at c) pH 6, d) pH 7.4 and e) pH 9. Lighter colors histograms in c, d and e show clean bubble - C. vulgaris cell interactions at the corresponding pH values.*

In a next step, to see how these interactions between cells and PO-chitosan bubbles influence cell capture and subsequent separation by the bubbles, we performed flotation experiments. To produce functionalized bubbles, water containing PO-chitosan was pressurized to 6 bar for 30 minutes. Then, by introducing the white waters into the flotation beakers, the bubbles and surfactants are released into the medium at the same time; since the surfactants are in close proximity to the bubbles, they can assemble on their surface. Figure 4a is a schematic representation of the flotation process with bubble functionalization, performed in only one step then with no prior flocculation. Unless otherwise indicated all the experiments were performed at pH 6. For that, in a first set of experiments, 50 mL of PO-chitosan white waters were injected from the pressurization tank to each beaker *via* the solenoid valves. Different PO-chitosan concentrations were tested in a range from 12.5 to 100 mg/L, and allowed to determine the best conditions, using 25 mg/L of PO-chitosan, where the highest separation efficiency was obtained (Supplementary Figure 3). Indeed, at low concentrations, for the volume of bubbles used, there is not enough PO-chitosan to coat the surface of bubbles resulting in poor flotation efficiency. On the contrary, when higher concentrations are used, there is too much PO-chitosan compared to bubbles, thus PO-chitosan molecules may end up in the suspension and saturate it, preventing bubbles to interact with cells.

To confirm this, we then used the best concentration obtained, 25 mg/mL of PO-chitosan, and varied the ratio of bubbles to cells. For that, we decreased or increased the volume of white waters injected in the microalgae suspensions; this results in a lower or higher number of bubbles and thus in a decreased or increased bubble surface area compared to cells. Four different injected white waters volumes were tested (20, 50, 80 and 100 mL); the results obtained are presented in Figure 4c. On this graph, the light blue bars correspond to the control conditions (clean bubbles) and the dark blue bars correspond to PO-chitosan coated bubbles. The highest separation efficiency was of 55.1 ± 13.1%, obtained with a white water volume of 50 mL, which is 1.6 times higher than the efficiency obtained with clean bubbles (34.6 ± 3.8%). The fact that using clean bubbles,

approximately 30% of the cells could be separated from the culture medium can result from the capture of cells by clean bubbles or from a natural flocculation of cells in these conditions followed by their capture by bubbles. Lower separation efficiencies, close the ones obtained in control conditions with clean bubbles, were found when using both lower volume (33.2 ± 2.8 % for 20 mL of bubbles) and higher volumes of bubbles (13.7 ± 1.9% and 12.6 ± 1.6% respectively for 80 and 100 mL of bubbles). The results obtained using 20 mL can be explained by the fact that in this case the surface area of the bubbles is not large enough compared to the amount of PO-chitosan available, which saturates the suspension and prevents the bubbles from interacting with cells. On the contrary, the poor results obtained using larger volumes may be due to too low a concentration of PO-chitosan relative to the bubbles, which are therefore not all functionalized with the surfactant, resulting in poor interaction with the cells. Furthermore, at these large volumes, the efficiencies obtained with clean bubbles also decrease, suggesting that injecting such volumes of bubbles dilutes the solution, resulting in a low probability of collision between bubbles and cells. Finally, as we found that cells' interactions with PO-chitosan coated bubble are dependent on the pH, we then investigated the influence of pH variation of the separation efficiency using 25 mg/L of PO-chitosan with an injected volume of white waters of 50 mL. The results presented in Figure 4c show that the highest separation efficiency of 55.1 ± 13.1% is obtained for pH 6, and decreases gradually to 38.6 ± 0.8% at pH 7.4 and to 27.3 ± 5.9% at pH 9. This is in line with the FluidFM experiments which showed higher interactions at pH 6, with average adhesion values decreasing then at pH 7.4 and pH 9. These experiments then prove that flotation efficiency using functionalized bubbles is dependent on the interaction that bubbles have with cells; the higher it is, the more efficient the separation process.

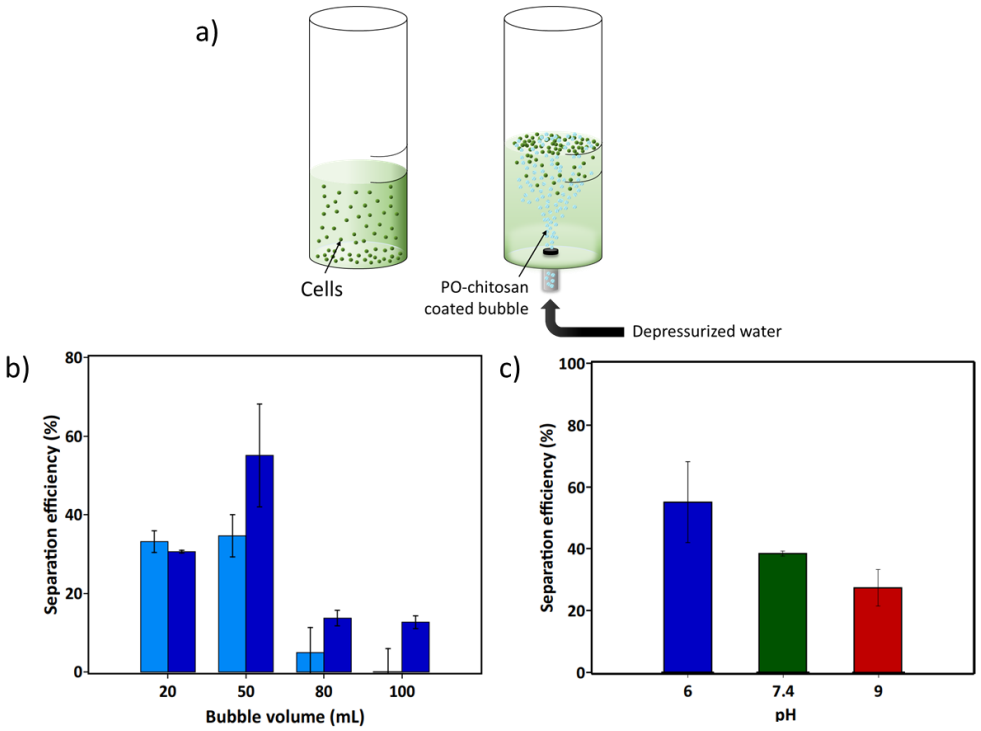

Figure 4: Flotation experiments of C. vulgaris with PO-chitosan coated bubble. *a) Schematic representation of one-step flotation experiments. b) Flotation efficiency of C. vulgaris with 25 mg/L PO-chitosan coated bubble with varying bubble volume at pH 6. Light blue bars correspond to the control condition with clean bubbles, and dark blue bars correspond to the test conditions with bubbles coated with PO-chitosan. c) Flotation efficiency of C. vulgaris with 25 mg/L and 50 mL PO-chitosan coated bubble at varying pH.*

The team of Henderson was the first to use functionalized bubbles to improve microalgae harvesting by flotation [31,32]. Their first studies on this topic showed that mixing cationic polymers with water in the saturator of a DAF unit allowed the production of positively-charged bubbles, which could then interact with negatively-charged microalgae cell surfaces and separate them without the need for prior flocculation. They then analyzed the effect of different polymers (different zeta potential and hydrophobic modifications with different groups) on the PosiDAF process and showed that while a change in the zeta potential had an influence on the interaction between polymers and bubbles, a change in the hydrophobic moieties incorporated in the different polymers affected the absorption conformation of polymers on the bubble surface [33]. They then tested these polymers in DAF experiments and showed that depending on the polymer used, the maximum removal efficiency stays more or less constant for the same species. However, depending on the species used, the removal efficiency varies; maximum removal efficiency was around 69% for *C. vulgaris*, while it was of 38% for a first strain of *Microcystis aeruginosa* and 93% for another strain of *M. aeruginosa* [33]. Then later they made the hypothesis that the separation efficiencies obtained were dependent on the algal organic matter (AOM) that cell produce, which differ depending on the species [34]. To test this hypothesis, they removed the AOM from cells and repeated the flotation experiment with positive bubbles: their results showed a decrease of the separation efficiencies for all species. Moreover, by substituting the AOM of one strain of *M. aeruginosa* CS-564/01 (the one for which the highest separation efficiency was obtained) with the second species of *M. aeruginosa*, the separation efficiency increased to 90%. This thus proved that AOM is indeed an important factor promoting the attachment of cells to the bubble surfaces [34]. In our case, the interactions between the PO-chitosan functionalized bubbles and the cells are not based on an electrostatic interaction, as discussed previously, but rather on a specific interaction between the chitosan backbone of the molecule, present on the surface of the bubbles, and the polymers on the surface of the cells. Thus, the very concept of the bubble functionalization strategy is different from the Posi-DAF process, but similar results could be obtained regarding cell separation. To also test the hypothesis that AOM could be involved in the interaction with PO-chitosan functionalized bubbles, we also performed the experiments with cells in stationary phase, under the conditions for which the best separation efficiency was obtained (pH 6 and 50 mL of injected bubbles). Cells in stationary phase have grown for a longer period of time (21 days instead of 7 for *C. vulgaris*), and have produced more AOM in the culture medium. In this case, the separation efficiency obtained was of 46.1 ± 9.2%, thus in the same range as for 7-days old cells. This means that in our case, AOM is most likely not involved in the interaction, unlike in the case of Posi-DAF and, as discussed earlier, relies on the specific interaction between chitosan and the cell wall of cells.

Another point that needs to be discussed here is the difference between the bubble functionalization strategy that we develop in this study and another flotation separation process called foam flotation. Foam flotation is a type of DiAF (Dispersed Air Flotation) where surfactants are mixed in the suspension to reduce the surface tension of water. Then bubbles are injected, allowing to create a stable foam where hydrophobic particles are adsorbed [35]. This process, which originates from the mineral industry [36], is also used for industrial waste water treatment [37] or plastic recycling [38]. For microalgae harvesting applications, foam flotation uses cationic surfactants (most often chemical surfactants) that not only stabilize the foam in the system but also enhance microalgae hydrophobicity, which is generally weak [39]. In both cases, cationic surfactants attach either to bubbles or cells which are both negatively-charged through electrostatic interactions, making the bubble surface positively-charged or the cell surface hydrophobic, allowing the interaction between the two entities. Thus the process we develop in this study is different from foam flotation, first because of the bubble generation procedure, different between DAF and DiAF

[40]. Second because no foam is generated in our process as PO-chitosan is not dispersed into the medium but mixed with water directly in the pressurization tank to produce functionalized bubbles. And third because the interaction between functionalized bubbles and cells is based on a specific interaction between the chitosan backbone at the surface of bubbles and polymers at the surface of cells and not on an electrostatic one. While the microalgae recovery rates can be higher in foam flotation than what is obtained here (up to 95% depending on the type of cationic surfactant used), such processes are usually performed using chemical flocculants (such as CTAB, DAH or DN2) which contaminate the biomass [41]. Bio-surfactants can also be used, such as rhamnolipid or saponin, but very few studies have reported on their efficient use for microalgae harvesting in foam flotation [41,42]. The advantage of the strategy we develop here is that chitosan is a bio-sourced molecule with no impact on cells, for which the mechanism of interaction with cells is known, making it possible to optimize the conditions for flotation. But when considering the concept of foam flotation, a question that can be asked is to know whether PO-chitosan mixed in the suspension could bind to cells, and act as an effective collector molecule that could enhance the hydrophobic properties of cells and promote their interactions with bubbles.

3.4. PO-chitosan is an efficient flocculant for *C. vulgaris* at different pH

To find some answers to this question, we next investigated the interactions of PO-chitosan directly with cells using AFM. For that, we used FluidFM technology, where single *C. vulgaris* cells were aspirated at the aperture of FluidFM probes by exerting a negative pressure inside the microfluidic cantilever, and further used as cell probes to measure the interactions with PO-chitosan surfaces. This FluidFM method, compared to classic single-cell force spectroscopy methods using AFM [43], has the advantage of keeping the cells stable on the cantilever even when in contact with a strongly adhesive surface [17]. In this case also the experiments were performed at different pH (6, 7.4 and 9), given the influence it has on PO-chitosan molecule. The schematic representation of these experiments is showed in Figure 5a, while the results obtained are presented in Figure 5b-d. At pH 6 (Figure 5b), the retract force curves obtained show a single retract peak happening close to the contact point, similar to what was observed with bubbles, this time with a smaller average force of 3.7 ± 1.3 nN (n= 2851 force curves with 6 cells coming from 2 independent cultures). As for the interactions with bubbles, this force signature is typical of non-specific interactions such as hydrophobic interactions. This first information is important. Indeed, previous results obtained by performing the same experiments with chitosan surfaces showed force curves with unfolding taking place far from the contact point, reflecting a specific interaction between chitosan and cell wall polymers [17]. This means that for PO-chitosan, the interaction is not based on the same mechanism: instead of a specific interaction with the chitosan backbone of PO-chitosan, it seems here that a hydrophobic interaction between the hydrophobic octanal groups added to the molecule and the cell surface is dominant. Thus by changing the molecule, we also changed the physico-chemical nature of its interactions with cells, and enhanced it as with PO-chitosan the interaction force is 10 times higher than for chitosan. Similar force curves were obtained at pH 7.4, with an average adhesion force of 3.2 ± 1.6 nN (n= 3194 force curves with 6 cells coming from 2 independent cultures, Figure 5c). Once we further increase the pH to 9 (Figure 5d), *C. vulgaris* interacts with PO-chitosan through the same mechanism (force curves present the same single retract peak at the contact point), but this time with a much lower adhesion force of 0.8 ± 0.6 nN (n= 2954 force curves with 6 cells coming from 2 independent cultures). Statistical analysis revealed that all differences are significant (unpaired t-test, p-value of 0.05) meaning that hydrophobic interactions are progressively suppressed with increasing pH. Now that we know that PO-chitosan interactions with cells are

dominantly hydrophobic, these difference observed at different pH can be easily explained. Indeed, at pH 9 for instance, both PO-chitosan and cells experience changes in their hydrophobic properties. While the WCA of PO-chitosan decreases to 44.6°, the surface of *C. vulgaris* cells becomes hydrophilic (no interactions with clean bubbles), and thus interacts less with PO-chitosan. These results are important because this means that PO-chitosan could not be used as a collector to enhance the hydrophobic properties of cells. Indeed, it interacts dominantly with cells *via* its hydrophobic groups, thus the chitosan backbone of the molecule is most likely present on the cell surface, making it probably even more hydrophilic. However, given the important adhesion forces obtained especially at pH 6 and 7.4, PO-chitosan could perhaps be efficiently used as a flocculant, which could also be an

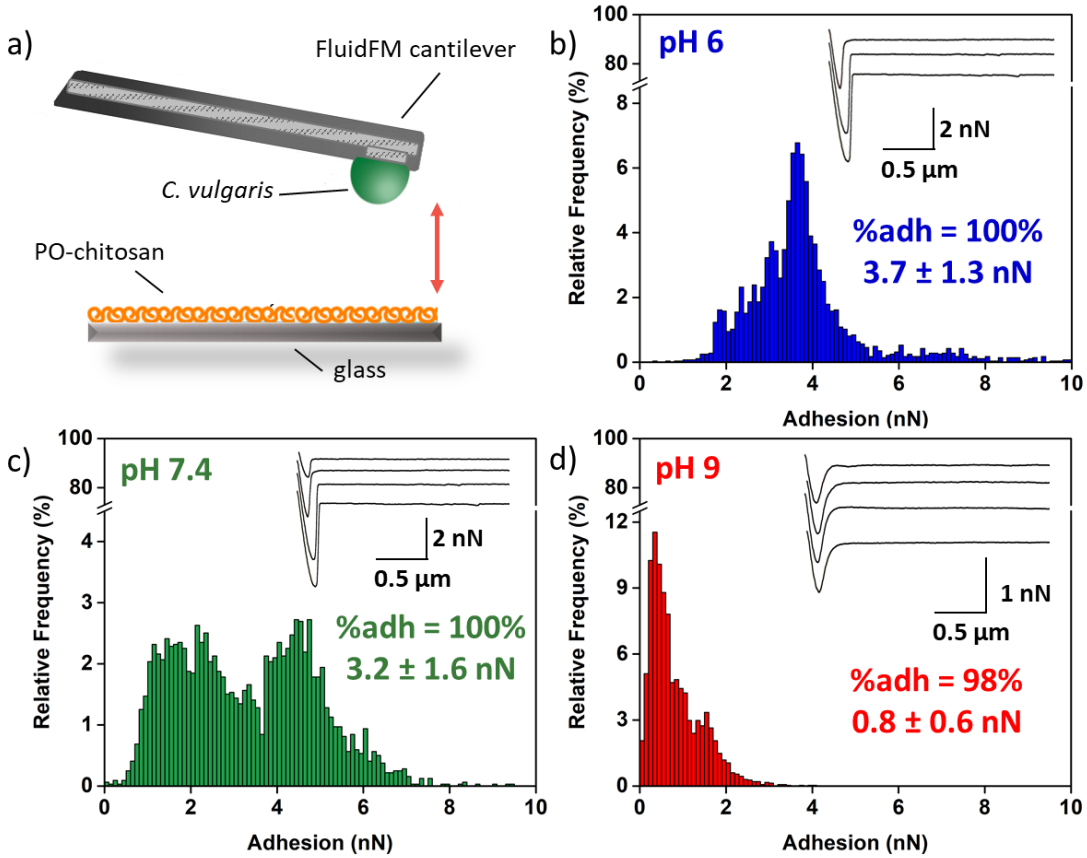

interesting aspect for harvesting.

Figure 5. Interaction between PO-chitosan and single C. vulgaris cells at varying pH. *a) Schematic representation of C. vulgaris and PO-chitosan coated surface interaction with FluidFM. Adhesion force histogram between C. vulgaris cells and PO-chitosan coated surface at b) pH 6, c) pH 7.4 and d) pH 9. Insets in panels show representative force curves obtained*

To test this hypothesis, we next conducted flocculation experiments with *C. vulgaris* cells at different pH with different PO-chitosan concentrations (Figure 6a). In these experiments, no bubbles are injected in the solution, cells are mixed with PO-chitosan and then left to settle for 30 minutes. The effect of PO-chitosan concentration on flocculation efficiency was first studied at pH 6 where the highest flotation efficiencies were reached; the results obtained are presented in Figure 6b. They show that for low concentrations of PO-chitosan, until 30 mg/L, flocculation efficiency increases with the dose of PO-chitosan used. The maximum flocculation efficiency was of 90.7 ± 0.5%, obtained at a concentration of 30 mg/L. However, for concentrations higher than 30 mg/L, flocculation efficiency

decreases dramatically and then reaches a plateau at 48 mg/L where the efficiency is close to 5%. This means that there is a concentration threshold at which the trend is reversed. Such tendency has already been observed in the case of chitosan, where for small concentrations (up to 10 mg/L) flocculation efficiency increases with increasing chitosan concentrations whereas for higher chitosan concentrations (greater than 20 mg/L) flocculation efficiency declines drastically [17,19]. This may be due to the fact that at high concentrations, the solution is saturated by the large quantity of molecules present in the microalgal suspension, interfering with their encounter with *C. vulgaris* cells and probably interacting with themselves rather than with cells. However in the case of chitosan, only low concentrations (10 mg/L) are needed to achieve high flocculation efficiencies [17]. The fact that PO-chitosan needs a higher dose to reach nearly 100% of flocculated cells is most probably due to the fact that PO-chitosan interacts with cells through its hydrophobic groups, which could substitute only 12% of the amine groups present in chitosan. Thus less groups are available for interactions, meaning that more molecules are needed to flocculate all cells. For the next experiments, we then chose to compare results obtained with 10 mg/L of chitosan and with 30 mg/L of PO-chitosan as these concentrations result in the highest flocculation efficiencies.

As for PO-chitosan coated bubbles, we then evaluated the effects of pH variations on flocculation efficiencies. The results obtained at pH 6, 7.4 and 9 are presented in Figure 6c. At pH 6 (dark bars), both chitosan (orange bars) and PO-chitosan (blue bars) resulted in high flocculation efficiencies: 95.2 ± 1.3% and 90.7 ± 0.5%, respectively. While flocculation efficiency decreases at pH 7.4 to 76.6 ± 2.4 % when using chitosan, it remains constant at 91.1 ± 2.6% for PO-chitosan (middle bars). However, once pH is further increased to 9 (light bars), flocculation efficiencies drop drastically to 11.1 ± 2.2% and to 10.0 ± 1.3% for both chitosan and PO-chitosan, respectively. In the case of chitosan, the situation can be easily explained by the fact that at higher pH, chitosan precipitates and does not interact with cells anymore. While there, a high flocculation can still be achieved as cells can get entrapped in the precipitate and flocculated by sweeping, this requires much higher concentrations of chitosan [16,17]. In the case of PO-chitosan, the situation is different since this molecule does not precipitate at high pH. But this decrease in flocculation efficiency can be easily explained by considering the results obtained by AFM, which showed that indeed at pH 9, the adhesion strength between PO-chitosan and the cells decreases significantly compared to pH 6 and 7.4. Another interesting part of these results concerns the control conditions (Figure 5c, green bars). Indeed, at pH 6, when no flocculant are used, cells are still able to flocculate with an efficiency of 33.2 ± 2.8%. This explains why in flotation experiments using clean bubbles, approximately 30% of the biomass can be separated. While cells can interact directly with clean bubbles through hydrophobic interactions (Figure 3c, light blue bars), the fact that they are able to flocculate naturally at this pH facilitate their collision with bubbles thereby making it possible to float them. However when the pH is increased to 7.4 and 9, no flocculation at all could be observed, meaning that cells cannot flocculate anymore naturally. Natural flocculation is often due to the production of EPS by cells: perhaps at elevated pH, the charge of these EPS changes, as it is the case for microbial EPS [44] thereby changing their interactions with cells.

Thus these results show that indeed PO-chitosan is an efficient flocculant for *C. vulgaris* cells at pH of 6 and 7.4, and that, as AFM results showed, because PO-chitosan is able to interact through hydrophobic interactions with cells. However, at these pH values, PO-chitosan molecule could still be positively charged (pKa of chitosan is of 6.5). Thus to confirm that the flocculation efficiencies observed at low pH are only due to hydrophobic interactions and not to electrostatic interactions between PO-chitosan and cells, we performed more experiments. First we measured the zeta potential of cells at pH 6, 7.4 and 9. The results obtained showed that *C. vulgaris* cells have an average zeta potential of - 27.1, -26.9 and -26.9 mV respectively. Thus, the global charge of *C.*

vulgaris cells is negative and does not change depending on the pH. This is a first element, as a change in the charge of cells may have explained the decreased flocculation efficiency obtained at pH 9, although PO-chitosan should not be positively charged at this pH. Second, we repeated the flocculation experiments and added 0.2 M of NaCl in the suspension at pH 6 to screen the charges present on cells and PO-chitosan molecules. The results obtained are presented at Figure 6d, they show similar flocculation efficiencies of 88.3 ± 1.1 %, 92.7 ± 2.9 % and 95.7 ± 0.1 % using PO-chitosan concentrations of 25, 30 and 40 mg/L. These results at the different concentrations are similar to what was obtained with no salts added (Figure 6b), showing that indeed, electrostatic interactions are not involved at pH 6. Finally we also performed flocculation experiments with stationary phase cells at pH 6, which we showed in another study are more hydrophobic than exponential phase cells because of the increase of the lipidic fraction in their cell wall upon aging [20]. The results obtained showed flocculation efficiencies of 44.7 ± 12.6% using chitosan and of 91.6 ± 0.9% using PO-chitosan (Supplementary Figure 4). In this case the reduced efficiency obtained using chitosan can be explained by the fact that the cell wall composition and architecture changes with growth [20]. As chitosan interaction with cells is a specific interaction [17], perhaps the polymers with which it interacts is less present at the surface of cells, resulting in less interactions and a decreased flocculation efficiency. The fact that using PO-chitosan, a similar flocculation efficiency is obtained with old cells further confirms that a different mechanisms is involved with this molecule, based, as AFM experiments showed, on hydrophobic interactions.

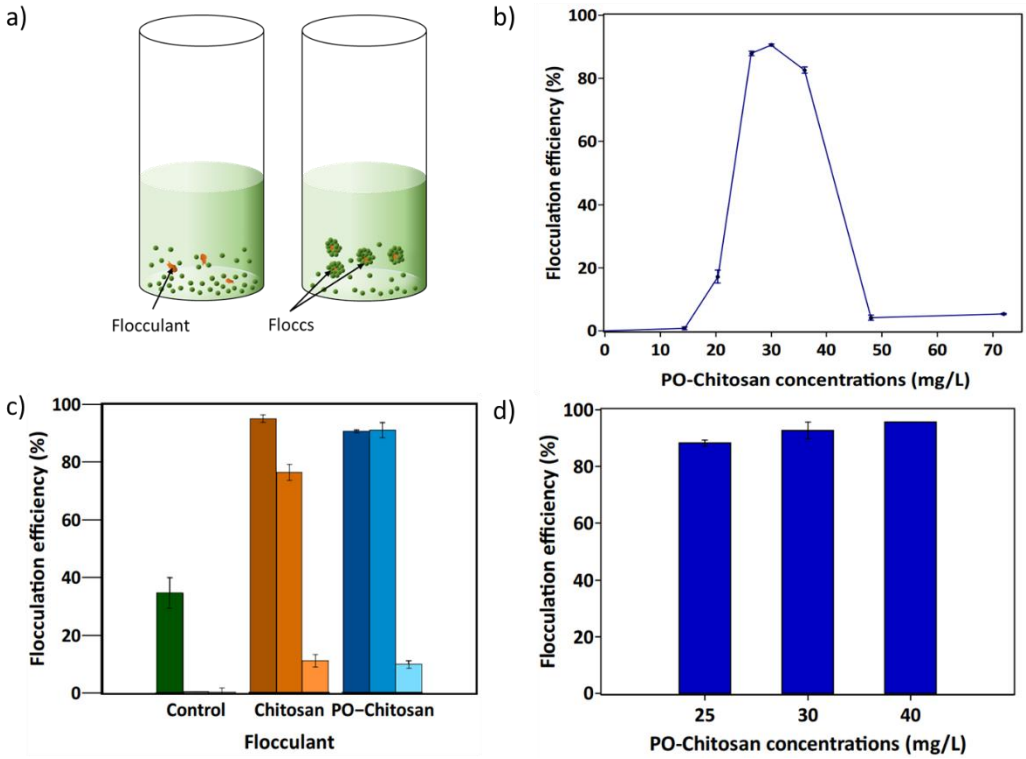

Figure 6. Flocculation experiments of C. vulgaris with PO-chitosan. *a) Schematic representation of flocculation experiments. b) Flocculation efficiency of C. vulgaris with varying PO-chitosan concentrations. c) Flocculation efficiency of C. vulgaris with 10 mg/L chitosan and 30 mg/L PO-chitosan with varying pH. Shades of the color indicates different pH. Darkest color represent the pH 6, medium color represent pH 7.4 and lightest color represent pH 9. d) Flocculation efficiency of C. vulgaris obtained with 25, 30 and 40 mg/L of PO-chitosan with 0.2 M of NaCl at pH 6.*

These results first show that PO-chitosan is also able to efficiently flocculate cells in a pH-dependent manner, as what was found with functionalized bubbles. Thus the interest of this molecule is in fact double, and depending on the process, it can be used either to harvest only part of the biomass using functionalized bubbles and leave cells to continue the culture, or to harvest the totality of the biomass using flocculation or flocculation/flotation in batch cultures. In flocculation, while the concentration of PO-chitosan needed is more important than for chitosan, it can however be used efficiently in more conditions compared to chitosan. First it is efficient at higher pH (7.4), which is quite important as *C. vulgaris* cultures usually reach pH values close to this in normal culture conditions. Thus using PO-chitosan, there is no need to first adjust the pH of the microalgae suspension, saving time and money in harvesting process. Second, it also allows flocculating stationary phase cells with high efficiency, which is also an important aspect as stationary cells can yield more of certain products, such as lipids [20]. Finally, another interesting aspect of PO-chitosan induced flocculation is the size of the flocs produced (see pictures in Supplementary Figure 5). For instance, using chitosan, cells aggregate into large flocs, that can be too heavy for microbubbles to carry them to the surface. Therefore using chitosan as a first step in a flocculation/flotation process may not be very efficient. However, the flocs obtained when using PO-chitosan are much smaller, probably because of the different flocculation mechanism involved, and can be carried up to the surface by the bubbles. Finally the originality of PO-chitosan as a flocculant is the fact that it interacts with cells via hydrophobic interactions. Indeed, most of the used bio-sourced flocculants for freshwater microalgae harvesting, including chitosan, interact with cells through electrostatic interactions, and flocculate cells through different mechanisms such as charge neutralization, bridging and patch mechanisms [13]. Examples of such flocculants are poly ϒ-glutamic acid (ϒ –PGA), a biopolymer produced by *Bacillus subtilis* [45], guar gum [14] or starch, a naturally-occurring polysaccharide [15]. Because microalgae cells usually have a weak hydrophobicity, most of the research has focused on these electrostatic interactions and cationic flocculants; hydrophobic interactions were never explored, as far as we know. But in fact, even if the hydrophobic properties of cells are weak, the hydrophobic interaction is a strong interaction (typically in the nN range), much stronger than electrostatic interactions (in the pN range). To give a concrete example of this, hydrophobic interactions can overcome an electrostatic repulsion between two entities, as we showed recently when probing the interactions between *C. vulgaris* cells and negatively-charged microplastic particles [28]. Thus even if the cell surface is slightly hydrophobic, this is enough to promote a strong interaction with a hydrophobic flocculant, which can result in high flocculation efficiencies like this is the case with PO-chitosan. In the end, this study, by revealing the potential of hydrophobic interactions to promote flocculation, shows that microalgae flocculation is not limited to positively charge biopolymers, and opens-up new avenues for finding new efficient flocculants.

4. Conclusions

Because microalgae harvesting is currently the most critical challenge for industry to exploit the full potential of this biomass, e.g. for biofuel production, new cost-effective solutions are needed. We propose here a new flotation harvesting process based on the functionalization of bubbles with a molecule that will improve their interactions with the cells. For this purpose, we based on previous knowledge on the interactions between chitosan and cells and modified this molecule with hydrophobic groups to make it amphiphilic. By characterizing this new molecule, we showed that PO-chitosan could be completely dissolved in water thanks to a low degree of substitution of the amine functions by the octanal groups of 12%, that indeed the modifications made conferred amphiphilic properties to the molecule, and that it does not precipitate at high pH unlike chitosan. We then used

this molecule to functionalize the surface of bubbles and probe their interactions with cells. As intended, the functionalization of bubbles allowed increasing in a significant manner their interactions with cells (from 3.5 to 12.8 nN at pH 6), in a pH-dependent manner. Further flotation experiments showed that flotation efficiency was directly correlated to the interaction between cells and functionalized bubbles, as flotation efficiency also changed with the pH. But in our best optimized conditions (pH of 6, 50% of injected white waters), the removal rate increased from approximately 30% with clean bubbles to almost 60%, demonstrating the efficiency of this new flotation process and its potential for continuous microalgae production systems where it could be used to harvest half of the cells and leave the remaining ones for continuing the culture. Then to see if PO-chitosan could also be used in different types of harvesting process, we also looked at its interactions directly with cells, and found that unlike chitosan, PO-chitosan interacts with cells though hydrophobic interactions, still in a pH-dependent manner. We thus tested its potential as a flocculant, and found that in fact PO-chitosan is an effective flocculant, able to flocculate nearly 100% of the cells in the suspension, in more conditions than chitosan, showing the interest of relying on hydrophobic interactions for flocculation. Here also, the efficiency was pH-dependent, in line with the results obtained using AFM. Altogether, this study presents an innovative flotation process in which the functionalization of bubbles with an amphiphilic chitosan allows enhancing cell capture and separation efficiency. In addition, we show that this molecule can also be used efficiently as a flocculant, making its interest double for large-scale harvesting applications. In each case, single-molecule level force spectroscopy experiments allow understanding the nature of the interactions, providing a complete view of the mechanisms involved and making it possible this way to optimize their use in large-scale applications.

Acknowledgements

C. F.-D. is a researcher at CNRS. C. F.-D. acknowledges financial support for this work from the Agence Nationale de la Recherche, JCJC project FLOTALG (ANR-18-CE43-0001-01). The authors want to thank Emma Regourd for her technical support on flocculation/flotation experiments and Abdlali Khalfaoui for constant assistance with the flotation device. In addition, the authors want to thank Dr. Juliette Fittreman from IMRCP laboratory in Toulouse for the loan of their AFM head while the one used for this study was under repair.

Conflicts of interest

The authors declare no conflicts of interest.

References

[1] N. Pragya, K.K. Pandey, P.K. Sahoo, A review on harvesting, oil extraction and biofuels production technologies from microalgae, Renewable and Sustainable Energy Reviews. 24 (2013) 159–171. https://doi.org/10.1016/j.rser.2013.03.034.

[2] M.I. Khan, J.H. Shin, J.D. Kim, The promising future of microalgae: current status, challenges, and optimization of a sustainable and renewable industry for biofuels, feed, and other products, Microbial Cell Factories. 17 (2018) 36. https://doi.org/10.1186/s12934-018-0879-x.

[3] L. Christenson, R. Sims, Production and harvesting of microalgae for wastewater treatment, biofuels, and bioproducts, Biotechnology Advances. 29 (2011) 686–702. https://doi.org/10.1016/j.biotechadv.2011.05.015.
[4] M.K. Lam, K.T. Lee, Microalgae biofuels: A critical review of issues, problems and the way forward, Biotechnology Advances. 30 (2012) 673–690. https://doi.org/10.1016/j.biotechadv.2011.11.008.
[5] J.J. Milledge, S. Heaven, A review of the harvesting of micro-algae for biofuel production, Rev Environ Sci Biotechnol. 12 (2013) 165–178. https://doi.org/10.1007/s11157-012-9301-z.
[6] Y.S.H. Najjar, A. Abu-Shamleh, Harvesting of microalgae by centrifugation for biodiesel production: A review, Algal Research. 51 (2020) 102046. https://doi.org/10.1016/j.algal.2020.102046.
[7] N. Uduman, Y. Qi, M.K. Danquah, G.M. Forde, A. Hoadley, Dewatering of microalgal cultures: A major bottleneck to algae-based fuels, Journal of Renewable and Sustainable Energy. 2 (2010) 012701. https://doi.org/10.1063/1.3294480.
[8] S. Garg, Y. Li, L. Wang, P.M. Schenk, Flotation of marine microalgae: Effect of algal hydrophobicity, Bioresource Technology. 121 (2012) 471–474. https://doi.org/10.1016/j.biortech.2012.06.111.
[9] D. Vandamme, I. Foubert, K. Muylaert, Flocculation as a low-cost method for harvesting microalgae for bulk biomass production, Trends in Biotechnology. 31 (2013) 233–239. https://doi.org/10.1016/j.tibtech.2012.12.005.
[10] H. Zhang, X. Zhang, Microalgal harvesting using foam flotation: A critical review, Biomass and Bioenergy. 120 (2019) 176–188. https://doi.org/10.1016/j.biombioe.2018.11.018.
[11] C. Yang, T. Dabros, D. Li, J. Czarnecki, J.H. Masliyah, Measurement of the Zeta Potential of Gas Bubbles in Aqueous Solutions by Microelectrophoresis Method, Journal of Colloid and Interface Science. 243 (2001) 128–135. https://doi.org/10.1006/jcis.2001.7842.
[12] S. Lama, K. Muylaert, T.B. Karki, I. Foubert, R.K. Henderson, D. Vandamme, Flocculation properties of several microalgae and a cyanobacterium species during ferric chloride, chitosan and alkaline flocculation, Bioresource Technology. 220 (2016) 464–470. https://doi.org/10.1016/j.biortech.2016.08.080.
[13] I. Demir, A. Besson, P. Guiraud, C. Formosa-Dague, Towards a better understanding of microalgae natural flocculation mechanisms to enhance flotation harvesting efficiency, Water Science and Technology. 82 (2020) 1009–1024. https://doi.org/10.2166/wst.2020.177.
[14] C. Banerjee, S. Ghosh, G. Sen, S. Mishra, P. Shukla, R. Bandopadhyay, Study of algal biomass harvesting using cationic guar gum from the natural plant source as flocculant, Carbohydrate Polymers. 92 (2013) 675–681. https://doi.org/10.1016/j.carbpol.2012.09.022.
[15] P.A. Hansel, R. Guy Riefler, B.J. Stuart, Efficient flocculation of microalgae for biomass production using cationic starch, Algal Research. 5 (2014) 133–139. https://doi.org/10.1016/j.algal.2014.07.002.
[16] J. Blockx, A. Verfaillie, W. Thielemans, K. Muylaert, Unravelling the Mechanism of Chitosan-Driven Flocculation of Microalgae in Seawater as a Function of pH, ACS Sustainable Chem. Eng. 6 (2018) 11273–11279. https://doi.org/10.1021/acssuschemeng.7b04802.
[17] I. Demir, J. Blockx, E. Dague, P. Guiraud, W. Thielemans, K. Muylaert, C. Formosa-Dague, Nanoscale Evidence Unravels Microalgae Flocculation Mechanism Induced by Chitosan, ACS Appl. Bio Mater. 3 (2020) 8446–8459. https://doi.org/10.1021/acsabm.0c00772.
[18] S. Ahmed, M. Ahmad, S. Ikram, Chitosan: A Natural Antimicrobial Agent- A Review, (2014) 11.
[19] A.L. Ahmad, N.H. Mat Yasin, C.J.C. Derek, J.K. Lim, Optimization of microalgae coagulation process using chitosan, Chemical Engineering Journal. 173 (2011) 879–882. https://doi.org/10.1016/j.cej.2011.07.070.
[20] I. Demir-Yilmaz, M. Schiavone, J. Esvan, P. Guiraud, C. Formosa-Dague, Combining AFM, XPS and chemical hydrolysis to understand the complexity and dynamics of C. vulgaris cell wall composition and architecture, (2022) 2022.07.11.499560. https://doi.org/10.1101/2022.07.11.499560.

[21] I. Demir-Yilmaz, P. Guiraud, C. Formosa-Dague, The contribution of Atomic Force Microscopy (AFM) in microalgae studies: A review, Algal Research. 60 (2021) 102506. https://doi.org/10.1016/j.algal.2021.102506.
[22] I. Demir, I. Lüchtefeld, C. Lemen, E. Dague, P. Guiraud, T. Zambelli, C. Formosa-Dague, Probing the interactions between air bubbles and (bio)interfaces at the nanoscale using FluidFM technology, Journal of Colloid and Interface Science. 604 (2021) 785–797. https://doi.org/10.1016/j.jcis.2021.07.036.
[23] J. Desbrières, C. Martinez, M. Rinaudo, Hydrophobic derivatives of chitosan: Characterization and rheological behaviour, International Journal of Biological Macromolecules. 19 (1996) 21–28. https://doi.org/10.1016/0141-8130(96)01095-1.
[24] N. Mati-Baouche, C. Delattre, H. de Baynast, M. Grédiac, J.-D. Mathias, A.V. Ursu, J. Desbrières, P. Michaud, Alkyl-Chitosan-Based Adhesive: Water Resistance Improvement, Molecules. 24 (2019) 1987. https://doi.org/10.3390/molecules24101987.
[25] J. Desbrieres, Autoassociative natural polymer derivatives: the alkylchitosans. Rheological behaviour and temperature stability, Polymer. 45 (2004) 3285–3295. https://doi.org/10.1016/j.polymer.2004.03.032.
[26] M. Yalpani, L.D. Hall, Some chemical and analytical aspects of polysaccharide modifications. III. Formation of branched-chain, soluble chitosan derivatives, Macromolecules. 17 (1984) 272–281. https://doi.org/10.1021/ma00133a003.
[27] J.L. Hutter, J. Bechhoefer, Calibration of atomic-force microscope tips, Review of Scientific Instruments. 64 (1993) 1868–1873. https://doi.org/10.1063/1.1143970.
[28] I. Demir-Yilmaz, N. Yakovenko, C. Roux, P. Guiraud, F. Collin, C. Coudret, A. ter Halle, C. Formosa-Dague, The role of microplastics in microalgae cells aggregation: A study at the molecular scale using atomic force microscopy, Science of The Total Environment. 832 (2022) 155036. https://doi.org/10.1016/j.scitotenv.2022.155036.
[29] A. Meister, M. Gabi, P. Behr, P. Studer, J. Vörös, P. Niedermann, J. Bitterli, J. Polesel-Maris, M. Liley, H. Heinzelmann, T. Zambelli, FluidFM: Combining Atomic Force Microscopy and Nanofluidics in a Universal Liquid Delivery System for Single Cell Applications and Beyond, Nano Lett. 9 (2009) 2501–2507. https://doi.org/10.1021/nl901384x.
[30] E. Dague, D. Alsteens, J.-P. Latgé, C. Verbelen, D. Raze, A.R. Baulard, Y.F. Dufrêne, Chemical Force Microscopy of Single Live Cells, Nano Lett. 7 (2007) 3026–3030. https://doi.org/10.1021/nl071476k.
[31] R.K. Henderson, S.A. Parsons, B. Jefferson, Surfactants as Bubble Surface Modifiers in the Flotation of Algae: Dissolved Air Flotation That Utilizes a Chemically Modified Bubble Surface, Environ. Sci. Technol. 42 (2008) 4883–4888. https://doi.org/10.1021/es702649h.
[32] R.K. Henderson, S.A. Parsons, B. Jefferson, Polymers as bubble surface modifiers in the flotation of algae, Environmental Technology. 31 (2010) 781–790. https://doi.org/10.1080/09593331003663302.
[33] N.R. Hanumanth Rao, A.M. Granville, C.I. Browne, R.R. Dagastine, R. Yap, B. Jefferson, R.K. Henderson, Determining how polymer-bubble interactions impact algal separation using the novel “Posi”-dissolved air flotation process, Separation and Purification Technology. 201 (2018) 139–147. https://doi.org/10.1016/j.seppur.2018.03.003.
[34] N.R. Hanumanth Rao, R. Yap, M. Whittaker, R.M. Stuetz, B. Jefferson, W.L. Peirson, A.M. Granville, R.K. Henderson, The role of algal organic matter in the separation of algae and cyanobacteria using the novel “Posi” - Dissolved air flotation process, Water Research. 130 (2018) 20–30. https://doi.org/10.1016/j.watres.2017.11.049.
[35] X. Nie, H. Zhang, S. Cheng, M. Mubashar, C. Xu, Y. Li, D. Tan, X. Zhang, Study on the cell-collector-bubble interfacial interactions during microalgae harvesting using foam flotation, Science of The Total Environment. 806 (2022) 150901. https://doi.org/10.1016/j.scitotenv.2021.150901.

[36] M.A.S. Barrozo, F.S. Lobato, Multi-objective optimization of column flotation of an igneous phosphate ore, International Journal of Mineral Processing. 146 (2016) 82–89. https://doi.org/10.1016/j.minpro.2015.12.001.
[37] D.S. Patil, S.M. Chavan, J.U.K. Oubagaranadin, A review of technologies for manganese removal from wastewaters, Journal of Environmental Chemical Engineering. 4 (2016) 468–487. https://doi.org/10.1016/j.jece.2015.11.028.
[38] C. Wang, H. Wang, J. Fu, Y. Liu, Flotation separation of waste plastics for recycling—A review, Waste Management. 41 (2015) 28–38. https://doi.org/10.1016/j.wasman.2015.03.027.
[39] M.A.S. Alkarawi, G.S. Caldwell, J.G.M. Lee, Continuous harvesting of microalgae biomass using foam flotation, Algal Research. 36 (2018) 125–138. https://doi.org/10.1016/j.algal.2018.10.018.
[40] J. Rubio, M.L. Souza, R.W. Smith, Overview of flotation as a wastewater treatment technique, Minerals Engineering. 15 (2002) 139–155. https://doi.org/10.1016/S0892-6875(01)00216-3.
[41] A. Krishnan, R. Devasya, Y. Hu, A. Bassi, Fundamental investigation of bio-surfactants-assisted harvesting strategy for microalgae, Biomass and Bioenergy. 158 (2022) 106364. https://doi.org/10.1016/j.biombioe.2022.106364.
[42] H.A. Kurniawati, S. Ismadji, J.C. Liu, Microalgae harvesting by flotation using natural saponin and chitosan, Bioresource Technology. 166 (2014) 429–434. https://doi.org/10.1016/j.biortech.2014.05.079.
[43] A. Beaussart, S. El-Kirat-Chatel, R.M.A. Sullan, D. Alsteens, P. Herman, S. Derclaye, Y.F. Dufrêne, Quantifying the forces guiding microbial cell adhesion using single-cell force spectroscopy, Nat Protoc. 9 (2014) 1049–1055. https://doi.org/10.1038/nprot.2014.066.
[44] L.-L. Wang, L.-F. Wang, X.-M. Ren, X.-D. Ye, W.-W. Li, S.-J. Yuan, M. Sun, G.-P. Sheng, H.-Q. Yu, X.-K. Wang, pH Dependence of Structure and Surface Properties of Microbial EPS, Environ. Sci. Technol. 46 (2012) 737–744. https://doi.org/10.1021/es203540w.
[45] H. Zheng, Z. Gao, J. Yin, X. Tang, X. Ji, H. Huang, Harvesting of microalgae by flocculation with poly (γ-glutamic acid), Bioresource Technology. 112 (2012) 212–220. https://doi.org/10.1016/j.biortech.2012.02.086.